Sensors and Materials, Vol. 37, No. 6 (2025) 2397–2408
MYU Tokyo

S & M 4062

Online Recognition of Human Gait Based on Smartphone Sensors

Song Li,* Yan Zhang, Xinzheng Huang, and Gong Lu

Intelligent System Laboratory of Qinghai University, Xining, Qinghai Province 810000, P. R. China

(Received February 12, 2025; accepted May 15, 2025)

Keywords: gait, smartphone sensors, online recognition, convolutional neural network, time domain features

To improve the accuracy of pedestrian gait recognition, a real-time recognition method for seven types of daily gait based on time domain features and a convolutional neural network is proposed. First, the acceleration and angular velocity sensors of the mobile phone are used to collect the time series data of the sensor on the x-, y-, and z-axes in the states of sitting, standing, walking, jogging, and squatting. The convolutional neural network is used for offline recognition, and the sampling times (t = 0.5, 1, and 1.5 s) are used for online real-time recognition. Then, two types of gait, ascending and descending stairs, are added for offline and online recognition and compared with the previous five types of classification recognition. We concluded that the gaits of walking and ascending stairs, as well as those of standing and descending stairs, are similar, which lead to the decrease in overall classification accuracy. Therefore, the time domain features of the total value of the acceleration sensor on the x-axis, the maximum change on the z-axis, and the change of steps during the sampling time are extracted, and the convolutional neural network model and time domain features are combined for online recognition. The experimental results showed that this method can significantly improve the transfer rate of gait recognition information and provide a new idea for gait recognition in the fields of motion detection and elderly monitoring.

1. Introduction

Pedestrian gait recognition, as an uncontrolled feature recognition method, is a new biometric recognition technology.(1) This technology is applied to not only motion detection, elderly monitoring, and indoor positioning, but also gradually to identity recognition, with broad application prospects.(2,3) At present, pedestrian gait recognition is mainly through image recognition and sensor recognition. Image recognition refers to collecting pedestrian gait images in public places through cameras, and then using machine learning technology for classification and recognition.(4,5) To accurately assess the health status of the elderly and provide appropriate care, Dou *et al.* proposed a continuous human activity recognition system, which uses the depth information obtained from multiple range-based depth cameras to generate a 3D human skeleton model, and on this basis, extracts the angle of human joints for daily life activity recognition,

*Corresponding author: e-mail: 2021990072@qhu.edu.cn
https://doi.org/10.18494/SAM5601

ISSN 0914-4935 © MYU K.K.
https://myukk.org/

with a recognition rate of 94.9% on the test set.(6) Del-Hoyo-Alonso *et al.* recognized common activities and 2D/3D body joints from input sources such as videos, image sets, or webcams, established a body flow library, and identified them using 2D and 3D pose estimation algorithms and three different human activity recognition models.(7) The recognition rate of the long short-term memory model was 90.4%, that of the convolutional neural network (CNN) model was 88.7%, and that of the transformer model was 91.3%.(7) Han *et al.* proposed a new human activity recognition method based on a visual converter.(8) Human activity recognition is realized using a multilayer perceptron classifier. The results showed that the method achieves the most advanced performance on three datasets.(8) Huo *et al.* proposed a dual-stream CNN based on a human contour deformation field to recognize human gait images, and the classification accuracy is up to 93.5% on the relevant dataset.(9) However, the above recognition is sensitive to the location of the camera and involves pedestrian privacy, so it cannot track and recognize pedestrian gait for a long time.

Sensor recognition refers to the use of wearable sensor devices to collect pedestrian gait data and machine learning technology to classify and recognize gait data.(10–12) Sezavar *et al.* proposed a deep neural network combining a group of convolution and capsule networks.(13) This structure uses a dynamic routing algorithm to train the capsule network, capture the equal variance with size and direction, and improve the classification efficiency of the model.(13) Kasubi and Huchaiah used wearable sensors to collect six types of human daily activity such as walking, going upstairs, going downstairs, sitting, standing, and lying, and then carried out feature extraction and classification. The classification accuracy of the support vector machine is up to 99.22%.(14) Qamar *et al.* used wearable sensors to solve the problem of position-independent human activity recognition and proposed a set of linear and nonlinear conversions of 3D sensor data to minimize the position and direction sensitivity of inertial sensors.(15) This method achieved the best average performance values of 94.7 and 91.7% in position-dependent and position-independent activity recognitions, respectively.(15) Dixon *et al.* proposed a new self-supervised learning method, namely, modal perception contrast learning, for the learning of multimodal sensor data and achieved good recognition performance on the open dataset.(16) Andersson *et al.* used the function of the smart phone inertial measurement unit and sensor fusion technology with accelerometer, gyroscope, and magnetometer data, and used various machine learning algorithms in a Weka environment to classify subjects, according to their hip joint patterns, with a classification accuracy of 88.9%.(17) Liu *et al.* proposed a high-precision and high real-time human behavior pattern recognition algorithm based on the time domain features of the outputs of accelerometers, gyroscopes, and barometers.(18) The algorithm selects the time domain eigenvalue of multisensor output as the unique feature and realizes the real-time recognition of behavior through feature extraction operation. The average recognition rate of eight human daily behavior patterns and four fall patterns can reach more than 94%.(18) Das *et al.* believed that the gait sequence is affected by the holding load, wearing type, shoe type, and so forth, and the collected data might be affected by covariate factors. Therefore, a new weighted multiscale CNN architecture was designed to extract local to global features to improve the recognition accuracy. A large number of experiments were carried out on four different benchmark datasets, and the demonstrated results of the proposed model are superior to other state-of-the-art deep learning approaches.(19) Abd Rahim *et al.* used smart phone inertial sensors to collect six human gait activities, namely, walking, going upstairs, going downstairs, sitting, standing, and lying, and they also used five types of integrated classifier for classification and recognition.(20) The accuracy rate of support vector machine was 99.22%, whereas the rf accuracy rate based on the random subspace integrated classifier was 97.91%.(20)

To sum up, image-based gait recognition is sensitive to the location of the camera layout and cannot track and recognize human gait for a long time. Compared with human gait recognition based on wearable sensors, it has the advantage of human gait recognition for a long time. However, if special sensors with fixed wearable positions are used, it will increase the research and development cost. As people become increasingly dependent on smart phones, using smart phone sensors to collect gait data and machine learning techniques can effectively reduce the research and development cost. Moreover, it is difficult to be applied in practice because most research studies are off-line gait recognition Therefore, this study has the following contributions: (1) an online real-time human gait recognition method based on an acceleration sensor and an angular velocity sensor is proposed, and (2) a method based on the time domain feature and CNN is proposed for online gait recognition, which improves the recognition rate.

2. System Construction and Data Preprocessing

Nowadays, smart phones are equipped with acceleration, angular velocity, orientation, and other sensors, so the smart phones carried by pedestrians can be used to collect gait data. However, owing to the differences between individual factors such as pedestrian height and weight, different pedestrian mobile phones are stored in different locations, which will affect the reliability of algorithm recognition. However, most people are used to placing mobile phones in the pants pocket. Therefore, six volunteers were recruited for this experiment, and their mobile phones were placed in their pants belt. The data collection diagram is shown in Fig. 1.

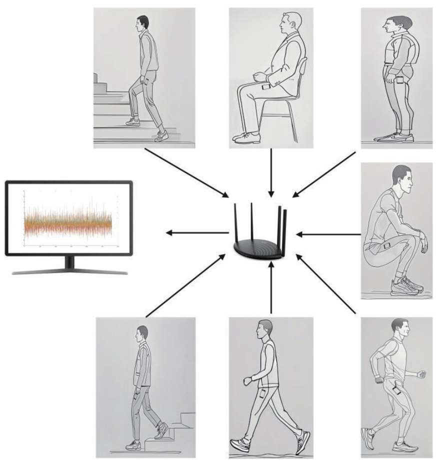

Fig. 1. (Color online) Data collection framework diagram.

The data acquisition system is composed of Matlab, Lan, and a mobile phone equipped with a Matlab mobile, which were built to collect the data of acceleration and angular velocity sensors on the three axes of volunteers in seven states: sitting, standing, jogging, walking, squatting, climbing, and descending stairs. The sampling frequency was 50 Hz. The schematic diagram of the three axes of the hand sensor is shown in Fig. 2.

During the training of the model, each volunteer collected 90 s of data in each state, kept the middle 60 s of data, and used the five-point cubic smoothing method to eliminate high-frequency random noise, as shown in Eq. (1).

$$\begin{aligned}
\overline{y_{t-2}} &= \left(69\times y_{t-2} + 4\times y_{t-1} - 6\times y_t + 4\times y_{t+1} - y_{t+2}\right)/70 \\
\overline{y_{t-1}} &= \left(2\times y_{t-2} + 27\times y_{t-1} - 12\times y_t + 8\times y_{t+1} - 2\times y_{t+2}\right)/35 \\
\overline{y_t} &= \left(-3\times y_{t-2} + 12\times y_{t-1} - 17\times y_t + 12\times y_{t+1} - 3\times y_{t+2}\right)/35 \\
\overline{y_{t+1}} &= \left(2\times y_{t-2} + 8\times y_{t-1} - 12\times y_t + 27\times y_{t+1} - 2\times y_{t+2}\right)/35 \\
\overline{y_{t+2}} &= \left(-y_{t-2} + 4\times y_{t-1} - 6\times y_t + 4\times y_{t+1} - 69\times y_{t+2}\right)/70
\end{aligned} \tag{1}$$

Here, $\overline{y_t}$ represents the smoothed values of acceleration and angular velocity at time t on a certain axis. Figures 3 and 4 respectively represent the smoothed data of acceleration and angular velocity for 60 s when volunteers walk, climb stairs, and descend stairs.

3. Related Algorithm

3.1 CNN

The CNN is a type of feedforward neural network with deep structure and convolution computation.[21] The CNN extracts local features of input data through convolution operation and forms a complex feature representation through multilayer convolution and pooling

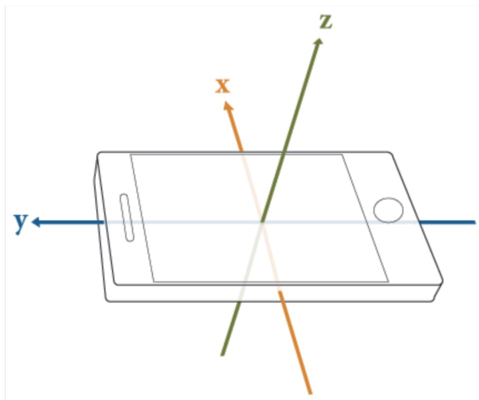

Fig. 2. (Color online) Schematic diagram of three-axis direction.

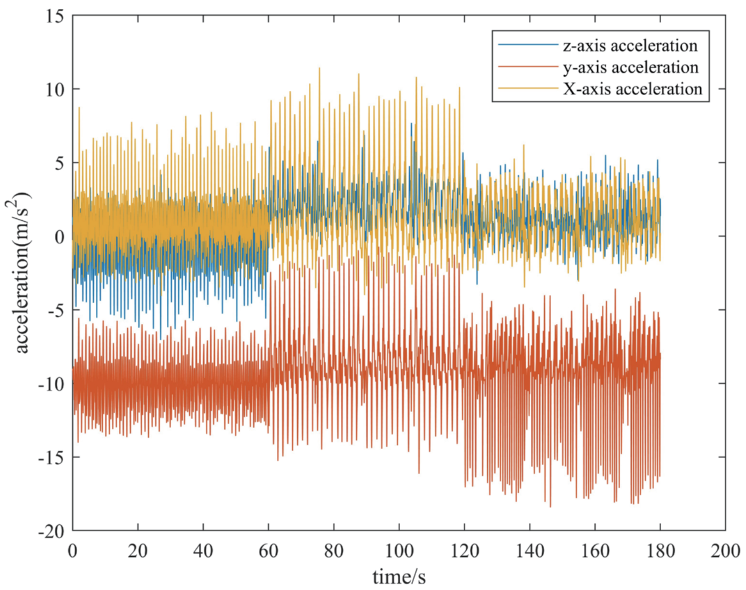

Fig. 3. (Color online) Smooth processing of raw acceleration data.

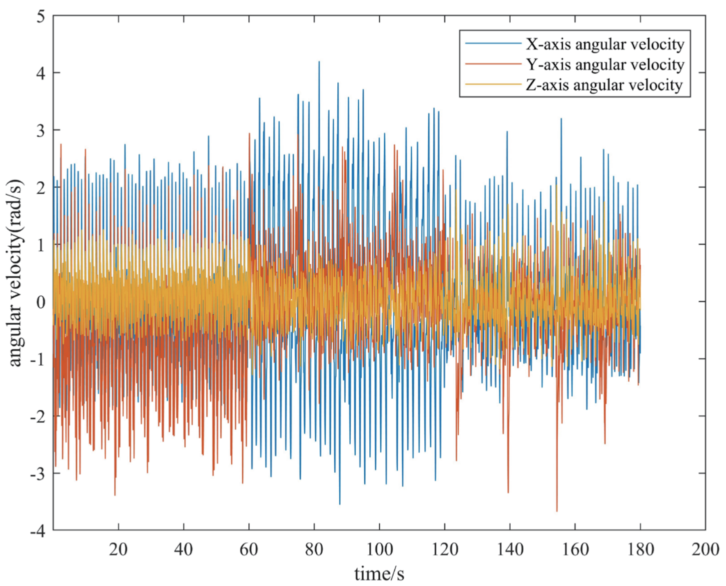

Fig. 4. (Color online) Smooth processing of raw angular velocity data.

operation. Finally, it carries out classification or regression tasks through the full connection layer. This design realizes feature extraction and classification through 1D convolution operation. The framework of feature extraction and classification of the 1D CNN is shown in Fig. 5. The input layer receives the preprocessed data and represents it as 1D sequence data. The convolution layer slides on the input data through the convolution kernel, calculates the dot product of the local region, and generates multiple features. Each convolution kernel can detect different features in the input data, as shown in the mathematical Eq. (2) of the convolution operation.

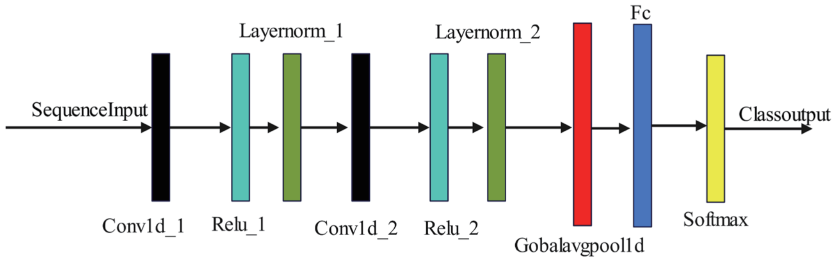

Fig. 5. (Color online) Schematic diagram of 1D-CNN framework.

$$(I\bullet K)(x,y)=\sum_{i=-a}^{a}\sum_{j=-b}^{b}I(x+i,y+j)\bullet K(i,j) \tag{2}$$

Here, I is the input data, K is the convolution kernel with a size of 6 × 6, (x, y) is the position on the output feature, a and b are the half height and half width of the convolution kernel, respectively, and the number of convolution kernels is determined by a genetic algorithm. After each convolution layer, a nonlinear activation function, such as a relu function, is usually applied to increase the nonlinear capability of the network. The relu function is calculated as

$$f(x)=\max(0,x)\,. \tag{3}$$

Layernorm is performed after two convolutions, that is, all neurons in a certain layer are normalized. It is mainly used to solve the problem of internal covariate offset in the training process, accelerate the convergence of the model, and improve the stability. The pooling layer is located behind the convolution layer. Its function is to downsample the data features, reduce the number of parameters and the amount of calculation while maintaining the important information of the features, and then use 1D global average pooling. Finally, the output of the softmax function is converted into a probability distribution, as shown in Eq. (4), and then the category with the highest probability is selected as the prediction category.

$$Soft\max(x_i)=\frac{e^{x_i}}{\sum_j e^{x_i}} \tag{4}$$

3.2 Time domain features

Time domain features are important parameters to describe the features of signals in the time domain. They can comprehensively reflect the time domain features of signals and provide an important basis for signal analysis and processing. The common time domain features include total value, mean value, variance, standard deviation, kurtosis, and absolute energy. The calculation is shown in Eqs. (5)–(8).

$$\sum_{i=1}^{n} x_i \tag{5}$$

$$\frac{1}{n}\sum_{i=1}^{n} x_i \tag{6}$$

$$\frac{1}{n}\sum_{i=1}^{n} (x_i - \bar{x}) \tag{7}$$

$$\frac{\frac{1}{n}\sum_{i=1}^{n} (x_i - \bar{x})^4}{\sigma^4} - 3 \tag{8}$$

In the above formula, X_i represents the sequence value of acceleration or angular velocity on a certain axis, and Eq. (5) represents the total sampling time, which is used to evaluate the overall size of real-time data. Equation (6) represents the mean real-time recognition time, which is used to evaluate the centralized trend of data. Equation (7) represents the variance in real-time recognition time, which is used to evaluate the centralized trend of data. Equation (8) represents the kurtosis within the real-time recognition time, which is used to evaluate the peak degree of the data. Among them, the number of steps is a very important feature in pedestrian gait recognition. The number of steps can be calculated by detecting the peak value of gait data and then the number of peaks in the corresponding time in the time domain. The peak value can also be directly used as the gait feature. The local maximum detection method is often used for peak detection, that is, the local maximum value is determined by comparing each data point with the point in its neighborhood.

4. Experimental Results and Analysis

In this experiment, the built gait real-time recognition system is used to collect the data every 2, 1, and 0.5 s. First, the data is smoothed and then sent to the convolutional neural network to classify and recognize the five gait types of sitting, standing, jogging, walking, and squatting using the trained model. The common classification accuracy and kappa values of the classification results of offline cross validation are shown in Table 1.

Table 1 shows that the accuracy of offline classification is above 97%, and the accuracy of volunteer 2's test set is as high as 99.86%. The kappa value of all volunteers is greater than 0.9, which indicates that the actual classification is almost consistent with the prediction results of the model, and also verifies the effectiveness of the five classification models.

In addition to accuracy, online real-time recognition is often evaluated using the information transfer rate (*ITR*). *ITR* refers to the amount of information output by the system per unit time, in bits/min. The results are shown in Table 2.

Table 1
Five types of gait offline classification result.

	Train set		Test set	
	Accuracy (%)	Kappa	Accuracy (%)	Kappa
Volunteer 1	99.04	0.98	97.97	0.97
Volunteer 2	99.94	0.99	99.86	0.99
Volunteer 3	98.52	0.98	97.93	0.97
Volunteer 4	98.96	0.98	98.24	0.98
Volunteer 5	98.60	0.98	98.02	0.97
Volunteer 6	99.81	0.99	99.71	0.99

Table 2
Real-time classification accuracies of five gaits at different sampling times.

Volunteer	t = 0.5 s		t = 1 s		t = 1.5 s	
	Accuracy (%)	*ITR*	Accuracy (%)	*ITR*	Accuracy (%)	*ITR*
Volunteer 1	85.40	2.86	86.93	1.50	98.33	1.44
Volunteer 2	81.34	2.50	94.04	1.87	99.45	1.51
Volunteer 3	79.71	2.37	90.35	1.67	92.59	1.19
Volunteer 4	84.76	2.80	93.18	1.82	99.47	1.51
Volunteer 5	83.89	2.72	91.34	1.72	93.79	1.24
Volunteer 6	89.30	3.28	93.18	1.80	96.83	1.37

Table 2 shows that the accuracy of real-time gait recognition in volunteer 5 gradually increases with the sampling time, indicating that the more information obtained, the higher the classification accuracy. When t = 0.5 s, the classification accuracy was above 80% except for volunteer 3. When t = 1 s, the classification accuracy was above 90% except for volunteer 1. When t = 1.5 s, the classification accuracy was above 92%, indicating the effectiveness of using the 1D CNN for the real-time recognition of the above five gait types. Because the five gait actions themselves are different, the recognition difficulty is small. Table 3 shows that when t = 1 s, the classification accuracy of each gait type, including sitting, squatting and running, is higher, but the recognition rates of standing and walking are slightly lower. It is possible that different volunteers are not completely stationary when standing, and there may be thigh jitter, leading to false recognition as walking. The lower classification accuracy of volunteers may be due to the fact that different volunteers walk with large amplitude and high frequency, which leads to false recognition as running, but the overall classification accuracy is higher.

However, in real life, the common gait also includes going up and down stairs. Because there is an elevator, people rarely go up and down stairs, but it is still necessary to add two types of gait for a total of seven types of gait for recognition. The offline identification results are shown in Table 4.

Table 4 shows that when adding two gaits of going up and down stairs for offline classification, a good offline classification effect can still be achieved by setting network parameters multiple times on the basis of experience. The lowest classification accuracy in the test set is 89.8%, and the highest can reach 96.10%. Then, with the trained model for online recognition, the recognition results are as shown in Table 5. Table 5 shows that after increasing

Table 3
Classification accuracies under different gaits at a sampling time of 1 s.

Volunteer	Sit (%)	Stand (%)	Crouch (%)	Run (%)	Walk (%)
Volunteer 1	100.00	78.04	86.60	100.00	70.00
Volunteer 2	100.00	92.30	96.50	100.00	81.40
Volunteer 3	75.38	82.50	97.70	100.00	96.29
Volunteer 4	100.00	82.50	97.70	100.00	85.70
Volunteer 5	100.00	96.00	96.70	100.00	64.00
Volunteer 6	100.00	95.00	90.90	100.00	80.00

Table 4
Seven types of gait offline classification result.

	Training set		Test set	
Volunteer	Accuracy (%)	Kappa	Accuracy (%)	Kappa
Volunteer 1	96.30	0.95	96.10	0.95
Volunteer 2	96.63	0.96	95.38	0.94
Volunteer 3	96.02	0.95	94.98	0.94
Volunteer 4	97.11	0.96	95.69	0.94
Volunteer 5	92.04	0.90	89.80	0.88
Volunteer 6	95.64	0.95	94.14	0.93

Table 5
Seven types of gait online classification result.

Volunteer	$t = 0.5$ s		$t = 1$ s		$t = 1.5$ s	
	Accuracy (%)	*ITR*	Accuracy (%)	*ITR*	Accuracy (%)	*ITR*
Volunteer 1	58.39	1.50	60.28	0.81	68.95	0.74
Volunteer 2	56.49	1.39	64.56	0.95	72.48	0.83
Volunteer 3	59.17	1.55	66.38	1.01	71.28	0.79
Volunteer 4	54.61	1.23	61.36	0.84	72.31	0.82
Volunteer 5	59.78	1.59	66.78	1.03	74.26	0.88
Volunteer 6	57.55	1.58	62.91	0.89	71.52	0.80

the number of categories to seven, the classification accuracy significantly decreases as compared with those of five categories, with the highest being only 74.26%.

Table 6 shows that the recognition of standing, walking, and going up and down stairs will be considerably affected after adding the two states of going up and down stairs. Because the gaits of walking and ascending stairs are very similar, and the gaits of standing and descending stairs are also similar, the accuracy of online recognition is reduced. Therefore, on the basis of the CNN classification, combined with time domain features, the second discrimination is proposed to improve the overall classification accuracy.

Figure 6 shows the data of a volunteer's acceleration on the *x*-axis time domain signal for 60 s when walking and going up and down stairs and the total value of time domain sampling every 1.5 s. From Fig. 6, we can see the difference in time domain feature between the total values of acceleration on the *x*-axis for 1.5 s when going up stairs and walking and going down stairs, so we can use this feature to distinguish going up stairs. At the same time, it is also possible to determine the number of steps that most people take when walking and going up and down

Table 6
Classification accuracies under different gaits at a sampling time of 1.5 s.

Volunteer	Sit (%)	Stand (%)	Crouch (%)	Run (%)	Walk (%)	Up the stairs (%)	Down the stairs (%)
Volunteer 1	100.00	42.00	93.30	90.00	62.50	48.88	46.00
Volunteer 2	96.15	55.55	95.00	85.71	73.20	46.00	55.76
Volunteer 3	93.30	54.50	96.60	81.25	58.00	53.30	62.06
Volunteer 4	95.00	43.33	96.00	93.33	75.00	41.40	62.12
Volunteer 5	100.00	41.17	95.45	85.00	75.70	48.33	74.19
Volunteer 6	100.00	33.00	92.85	85.00	80.00	45.40	64.40

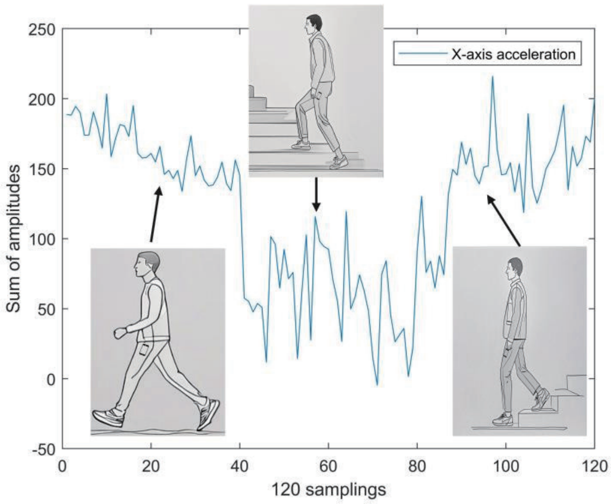

Fig. 6. (Color online) Total value of acceleration x-axis

stairs. In general, the speed of most people when walking is greater than that when going up and down stairs. As shown in Fig. 7, the number of steps when walking is greater than that when going up and down stairs at the same time. Therefore, this feature can be used to distinguish the gaits of walking and going up and down stairs.

Sometimes when standing, the legs are not completely static, and occasionally, there is the phenomenon of shaking the legs. To overcome the misunderstanding that the standing state is in the walking state, the change in the maximum value of the acceleration sensor on the z-axis within the sampling time can be extracted, as shown in Fig. 8. It can be seen from the figure that there are clear differences in the acceleration signals on the z-axis when volunteers are standing, walking, and going up and down stairs. The first 40 samples are the z-axis signals of standing, and the last 140 samples are the z-axis signals of walking and going up and down stairs.

By combining the time domain features and CNN model to classify seven types of gait, the results are shown in Table 7, which shows that the classification accuracy is improved under different sampling times, which verifies the effectiveness of the combination of time domain features and a neural network for seven types of gait recognition. Compared with existing studies, this research differs in both the types and quantity of gait patterns identified. While prior works[14,20] focused on six gait types, our study incorporates two additional patterns (jogging and squatting), expanding the recognition to seven gait types. This enhancement aligns

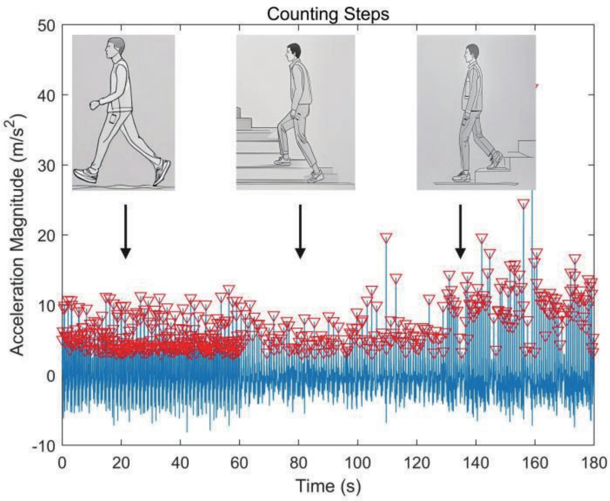

Fig. 7. (Color online) Step count statistics.

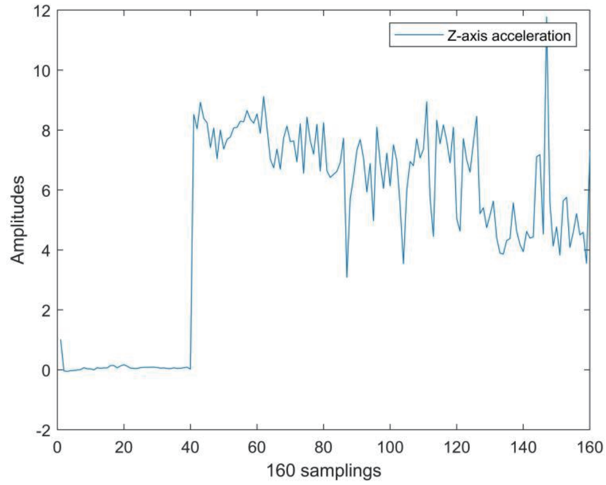

Fig. 8. (Color online) Maximum value of the z-axis acceleration signal every 1.5 s.

Table 7
Seven types of online gait classification result.

Volunteer	t = 0.5 s		t = 1 s		t = 1.5 s	
	Accuracy	*ITR*	Accuracy	*ITR*	Accuracy	*ITR*
Volunteer 1	82.43	3.36	88.36	1.98	90.11	1.39
Volunteer 2	80.81	3.21	91.47	2.16	92.58	1.49
Volunteer 3	78.58	3.00	89.76	2.06	90.33	1.39
Volunteer 4	82.37	3.35	91.46	2.16	92.28	1.47
Volunteer 5	85.83	3.70	92.74	2.24	93.45	1.52
Volunteer 6	90.84	4.26	90.16	2.08	91.55	1.44

better with daily human activities and increases practical relevance. Moreover, we implemented online gait recognition with varying sampling intervals, achieving recognition rates exceeding 90% at t = 1.5 s. In contrast, previous research primarily relied on offline recognition methods.

These innovations make our proposed gait recognition approach more applicable to real-world scenarios, providing new insights for transitioning gait recognition technology from laboratory environments to practical implementations.

5. Conclusions

To improve the accuracy of online gait recognition, we used the acceleration and angular velocity sensors of smart phones and people's habit of putting mobile phones in their pants pockets to collect the gait information of volunteers. The classification accuracies of five types of gait and seven types of gait under CNN were compared and analyzed, and a method combining time domain features and CNN was proposed. This method significantly improves the accuracy of the real-time classification of seven types of gait and provides a new idea for gait recognition in motion detection, elderly monitoring, and other fields.

Acknowledgments

Special thanks go to one of the authors of this article, Mr Huang, who has put considerable time and effort into checking the comments on the draft.

References

1 R. Veenu and M. Kumar: Multimedia Tools Appl. **82** (2023) 37003. https://doi.org/10.1007/s11042-023-15079-5
2 M. Khaliluzzaman, A. Uddin, K. Deb, and M. J. Hasan: Sensors **10** (2023) 4875. https://doi.org/10.3390/s23104875
3 J. Sena, J. Barreto, C. Caetano, G. Cramer, and W. R. Schwartz: Neurocomputing **444** (2021) 226.
4 L. Yao, W. Kusakunniran, Q. Wu, and J. Zhang: PeerJ Comput. Sci. **7** (2021) 382. https://doi.org/10.7717/peerj-cs.382
5 D. Zhu, L. Ji, L. Zhu, and C. Li: Int. J. Mach. Learn. Cybern. **15** (2024) 3791. https://doi.org/10.1007/s13042-024-02120-8
6 W. Dou, A. S. Azhar, W. Chin, and N. Kubota: Sens. Mater. **11** (2024) 4713.
7 R. Del-Hoyo-Alonso, A. C. Hernández-Ruiz, C. Marañes-Nueno, I. López-Bosque, R. Aznar-Gimeno, P. Salvo-Ibañez, P. Pérez-Lázaro, D. Abadía-Gallego, and M. Rodrigálvarez-Chamarro: Sensors **20** (2024) 6729.
8 H. Y. Han, H. W. Zeng, L. Q. Kuang, H. Xie, and H. G. Xue: Sci. Rep. **14** (2024) 15310.
9 W. Huo, K. Wang, J. Tang, N. Wang, and D. Liang: J. Electron. Inf. Technol. **46** (2024) 4062.
10 B. Bat-Orgil and J. L. Saver: J. Stroke Cerebrovascular Dis. **30** (2021) 105826.
11 S. Mekruksavanich and A. Jitpattanakul: Sensors **21** (2021) 7519. https://doi.org/10.3390/s21227519
12 A. P. Creagh, F. Lipsmeier, M. Lindemann, and M. D. Vos: Sci. Rep. **11** (2021) 14301. https://doi.org/10.1038/s41598-021-92776-x
13 A. Sezavar, R. Atta, and M. Ghanbari: Pattern Recognit. **147** (2024) 110054.
14 J. W. Kasubi and M. D. Huchaiah: Proc. 2021 Artificial Intelligence and Sustainable Computing for Smart City Conf. **1434** (2021) 282.
15 N. Qamar, N. Siddiqui, M. Ehatisham-ul-Haq, M. A. Azam, and U. Naeem: Procedia Comput. Sci. **177** (2020) 196.
16 S. Dixon, L. Yao, and R. Davidson: Concurrency Comput. Pract. Exper, **36** (2024) e8020.
17 R. Andersson, J. Bermejo-García, R. Agujetas, M. Cronhjort, and J. Chilo: Sensors **24** (2024) 4769. https://doi.org/10.3390/s24154769
18 Y. Liu, H. Y. Jiang, S. L. Wang, and Y. P. Chen: J. Shanghai Jiao Tong University (Science) **2** (2015) 169.
19 S. Das, S. Meher, and U. K. Sahoo: Sensors **22** (2022) 3968. https://doi.org/10.3390/s22113968
20 K. Abd Rahim, I. Elamvazuthi, L. Izhar, and G. Capi: Sensors **18** (2018) 4132. https://doi.org/10.3390/s18124132
21 Z. Li, F. Liu, and W. Yang: IEEE Trans. Neural Networks Learn. Syst. **33** (2021) 6999.